scientific reports

Check for updates

OPEN

Validated low-cost standardized VICON configuration as a practical approach to estimating the minimal accuracy of a specific setup

Adam Chromy[1,2]✉, Petr Sopak[1,2] & Hynek Cigler[3]

Motion Capture (MoCap) is rapidly growing in the sports, biomechanics, healthcare, and medicine segments, where accuracy is crucial. Current research studies are concurrently confirming that the accuracy can be determined *only for the specific analyzed configuration* and thus recommending performing your own accuracy verification on your specific setup. However, it is often hard to perform since it requires significant effort, time, knowledge of statistical data analysis and often equipment and tools that are not commonly available. This paper deals with this by creating a *standardized setup with carefully evaluated accuracy*, substituting the on-site validation process (in case of using such a setup) or providing the worst-case accuracy (when a more advanced setup is used). The setup is designed to be low-cost, easily reproducible and cover a wide range of applications – thus VICON setup with five VERO v1.3 cameras is used. The accuracy was evaluated using the robotic manipulator EPSON C3, determining that the absolute positioning accuracy of such a standardized setup is 0.65 mm on average (SD = 0.48, with maximal error of 2.47 mm) and rotation accuracy 0.40° (SD = 0.35, with maximal error of 2.0°), which is negligible considering the experimental diameter of 1.4 m and full angular span. The major source of error was specific to particular spatial and rotational positions; other systematic and other random errors were noticeably smaller. If the standardized setup is used and all its requirements are met, a similar accuracy as validated above can be expected without the need to explicitly validate the specific configuration, which is time-consuming and resource-intensive.

Keywords VICON, Motion capture, Validation, Accuracy assessment, Standardization

Optical motion tracking, also known as motion capture (MoCap), is a popular method to capture and analyze the movement of objects or people accurately; being primarily used in the entertainment industry, sports and biomechanics, healthcare and medicine, robotics and engineering or research[1]. It is a rapidly growing market (expected CAGR of 15% from 2024 to 2029[2]), expanding predominantly in the segments of sports, biomechanics, healthcare and medicine, where precision and accuracy are absolutely crucial factors[3].

Due to the principles of the MoCap measurement system, its accuracy cannot be established universally for a given measurement range, as it is common in other measuring instruments.

There are several studies that focus on analyzing the accuracy of MoCap systems in various application backgrounds.

Barrows[4] used Vicon MX-F40 cameras with markers on a 58 cm long rail, allowing the researchers to move the markers precisely. Windolf et al.[5] used a precise linear three-axis robot with absolute encoders to validate the Vicon 460 system accuracy, but only in a small volume ($0.18 \times 0.18 \times 0.15$ m); Yang et al.[6] investigated accuracy by comparing the captured movement of the markers with reference movement in similar volume. Merriaux et al.[7] repeated the experiment in a larger volume ($2 \times 1.5 \times 1$ m) with the larger linear three-axis robot and added dynamic assessments. Aurand et al.[8] extended the volume to $10.4 \times 6.5 \times 2$ m, but having only the 0.1 m long linear motion stage, they evaluated more precision at several places than the absolute accuracy of the system. They also demonstrated the influence of the camera number and distance. Hu et al.[9] performed very similar experiments in the smaller volume using linear motion induced by a precise micrometer, and Liu et al.[10] used a wedge comparator.

[1]CEITEC—Central European Institute of Technology, Brno University of Technology, Purkynova 656/123, 612 00 Brno, Czech Republic. [2]Faculty of Electrical Engineering and Communications, Brno University of Technology, Technicka 3082/12, 616 00 Brno, Czech Republic. [3]Psychology Research Institute, Faculty of Social Sciences, Masaryk University, Jostova 10, 602 00 Brno, Czech Republic. ✉email: chromy@vut.cz

The studies mentioned above[4–9] agree that the determined accuracy is only relevant for the specific analyzed setup, and many factors significantly affect the system's final accuracy (such as the number, placement, and orientation of cameras, as well as the appearance of the surrounding environment); so their main benefit is more the protocol for accuracy quantification than the accuracy analysis, despite the fact, they are presented.

Being aware of this, Eichelberger et al.[11] designed a simple and practical protocol for more detailed validation of a particular setup, using only standard laboratory equipment and providing trueness, precision and uncertainty of an installed system. Their work also pointed out that dynamic accuracy cannot be predicted based on static error assessments; the relationship between the speed and tracking error was also studied in[7] and[12], where the conclusion indicates that the closer the cameras are to the tracked object, the better the motion capture setup performs.

There is also more research on the topic[13–16], but since they do not use any positioning ground truth systems, they are irrelevant to our work.

To summarize, a common problem in all state-of-the-art research is the fact that to quantify the accuracy of our *specific* setup for our *particular* research; we need to *always* conduct a validation procedure, which, although well-described in the current literature, requires significant effort, time, knowledge of statistical data analysis, and often equipment and tools that are not commonly available. All of this is often not possible to carry out for various reasons, leading to situations where the accuracy of measurements for a given setup is not quantified, and a question hangs over the entire study as to whether the measurement error is not greater than the observed differences in the data. There is a lack of a standardized setup with verified accuracy, which would substitute the validation process.

Thus, the goal of this paper is to define a low-cost, standardized MoCap setup using the readily available equipment in a minimal (and thus less expensive) configuration, which is easily reconstructible. The accuracy of this setup was carefully verified and quantified in this paper, using the accurate robotic manipulator as a ground truth.

If a researcher sets up the same configuration and follows the defined criteria, they will know the measurement accuracy of their MoCap system setup without having to carry out cumbersome and demanding verifications. This paper also includes an analysis summarizing the factors that increase measurement accuracy. Thus, the applicability of accuracy results is not limited to this standardized setup only but can also be applied to *more advanced* configurations that meet the conditions outlined here. In these cases, their accuracy is not quantified exactly, but it can be inferred that it will certainly be better than what is stated here, which may be sufficient in many instances.

Materials and methods

Various motion capture technologies exist, each with different trade-offs in terms of cost, accuracy, and usability. Inertial systems are relatively affordable and easy to deploy, but they suffer from drift, magnetic interference, and lack of global positional accuracy, which limits their use for precise validation[17]. Markerless systems offer simple setup and user comfort but rely on computer vision algorithms and are known to have lower accuracy, especially under occlusion or dynamic motion[18].

Marker-based optical systems remain the most accurate solution for 3D tracking, especially in laboratory conditions. Our goal was to define a minimal optical configuration that still provides reliable accuracy. Therefore, we used five VICON VERO v1.3 cameras — four placed symmetrically to reconstruct the volume and one added to reduce occlusions during complex movements. This setup reflects a practical balance between cost, reproducibility, and performance.

Compared to alternative optical systems, such as OptiTrack, VICON VERO was chosen due to its wider availability in research environments and full integration with the VICON ecosystem. Although it offers lower resolution than high-end models, its performance is sufficient for defining an entry-level baseline setup with clearly validated accuracy.

In this section, we first define the standardized setup and the conditions that need to be met; then, we proceed to describe the procedure and implementation of verifying the accuracy of such a standardized setup.

Standardized VICON setup

Camera model

According to[2], VICON Motion Systems is the key player in the optical MoCap market, and their VICON VERO camera is their most sold product. It is produced in two different resolutions – 1.3MP (v1.3) and 2.2MP (v2.2). Although it has been shown that the higher resolution increases the accuracy[12,19], in our setup, we used VICON VERO v1.3 cameras with lower resolution in a wide FOV configuration. These cameras are more widespread, cost-effective, and well-suited for defining a reproducible and affordable baseline configuration. As such, the reported accuracy can be considered a representative entry-level baseline for MoCap systems that follow the defined spatial and visibility conditions. More advanced systems using higher-resolution cameras or more-cameras setups can be expected to achieve at least similar or better accuracy, but their performance is not quantified in this study, as the focus remains on a minimal low-cost configuration.

Covered volume

Focused on affordable solutions, we chose a covered volume of $4.17 \times 3.45 \times 2.89$ m, which is usually sufficient for moving body analysis or limited UGV/UAV operations (what are the most frequent usages of VICON[3]). According to Fig. 1, it leads to the $6.8 \times 5.0 \times 2.9$ m of occupied space, which is a volume which fits in the average-size rooms.

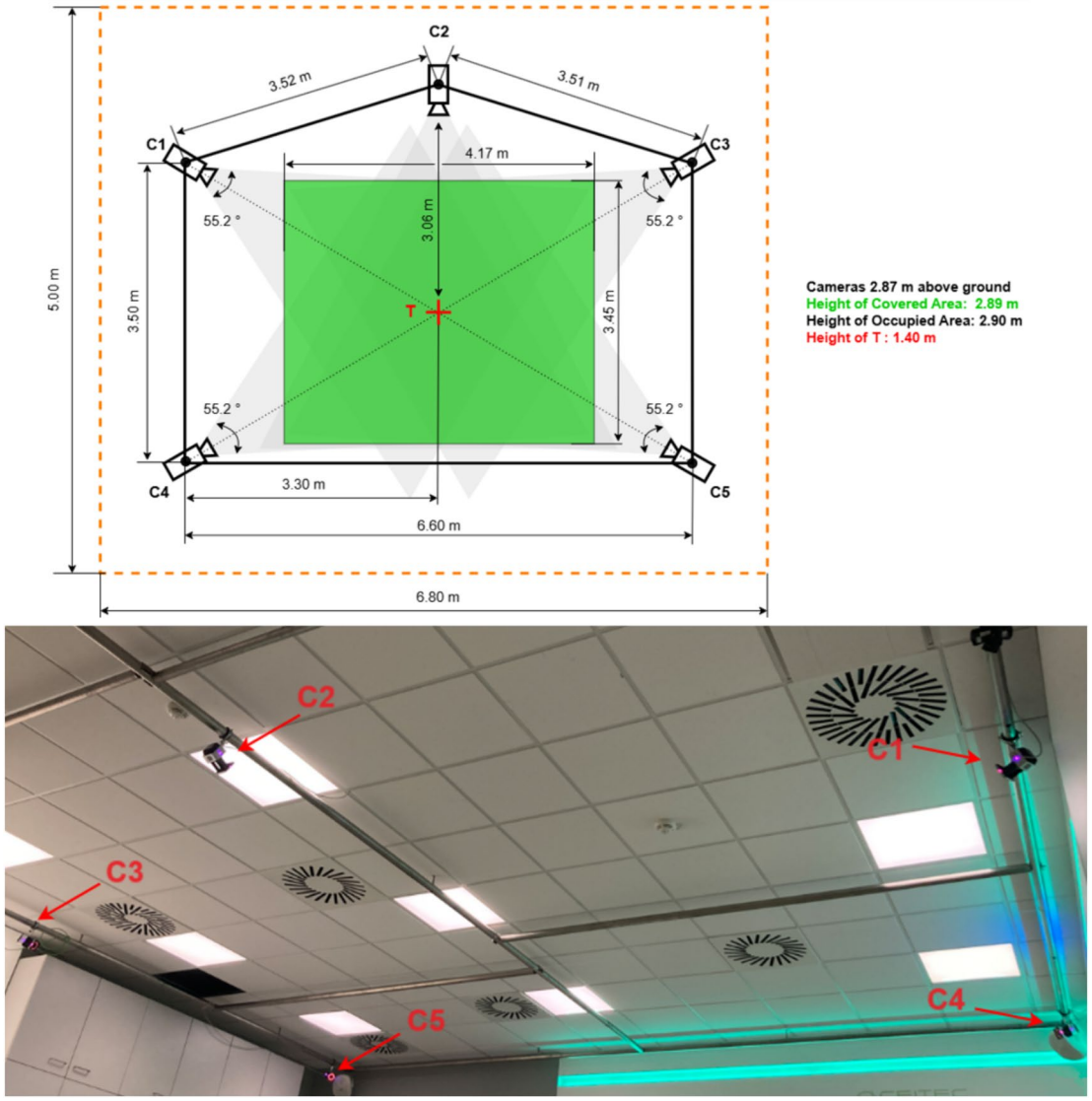

Fig. 1. Covered volume and placement of the cameras within the Standardized setup.

Number of cameras

Data from at least two cameras simultaneously is required to produce 3D reconstructions of the VICON markers, so the minimal number of cameras to cover a cubic area is 4; to maintain the tracker visibility during advanced body motion, 8 cameras are recommended[20]. According to Nagymate et. Al.[21], the most common number of cameras in the setups is 6, so we chose the setup with 4 symmetric cameras with one additional front-side camera, as shown in Fig. 1. The fields of view of the cameras overlapped so that the tracked markers were monitored by at least two cameras. The distance of the cameras is designed to be sufficiently close to the measured object to ensure high accuracy of measurement[8], simultaneously keeping sufficient space for moving the human body or limited UAV/UGV operations without the need to increase the number of cameras. According to our validation, the influence of the 5th camera on the accuracy when the tracker is visible also on the other 2 cameras is negligible, and it helps to avoid loss of view during the advanced body motions performed facing the 5th camera. Such a compromise ensures the low cost of the system and the ability to capture complex body motions simultaneously.

Cameras placement

The cameras must be mounted in a rigid position facing towards the centre point T. The height of T was set to 1.40 m to optimally enclose the Covered Area. This height is approximately the centre of the upper part of a human body; thus, we can expect it as the centre of most scenes. In our setup, the metallic frame connected to the ceiling was used as a base for camera holders.

VICON settings
In the VICON application, the Frame Rate was set to 100 Hz. For each camera, the GrayScale Mode was set to Auto, with Enabled LEDs, and the Strobe Intensity was set to 1. The cameras were configured to Wide mode (55.2 × 43.9°).

Trackers
Based on our literature review, measurement setups that include rotations are significantly more common. Since rotation tracking requires a multi-point marker, we excluded the single Pearl Marker localization from the setup, and adopted the multi-point trackers, which are supplied by the manufacturer (Fig. 3a). However, the results of this paper related to the position accuracy can be applied also to the single Pearl Marker localization (in such case, the rotational accuracy is not relevant).

Other constraints
There must be no shiny (reflective) objects similar to the trackers in the room since they can influence the system's accuracy. This can be checked during the VICON calibration – there should be no necessity to mask out some objects. Additionally, the lighting conditions must be kept constant throughout all experiments and only artificial ceiling lights shall be used, with no influence of daylight or flickering sources. Moreover, the manufacturer recommendations for proper use must be fully satisfied, for example the floor must not be reflective, etc.

Accuracy validation procedure

The accurate six-axis robotic manipulator EPSON C3 with a repeatability of ± 0.02 mm[22] was used as a source of reference values (ground truth) since it provides more accurate positioning data than is expected of the VICON system.

An original VICON Rigid Body tracking plate with four tracking marker balls was used in a manufacturer's recommended configuration of balls. We used configuration nr. 3, but they shall be equal. The tracker was attached to the endpoint of the manipulator, which was monitored during the experiment (Fig. 2).

The manipulator with the markers performed two types of movements according to predefined trajectories. This couple of movements was repeated four times; between each trial, the calibration of the VICON system was performed again. So finally, there were 16 datasets available – 8 for each of 2 calibrations, 4 with rotational trajectory and 4 with positional trajectory (see further).

The Vicon Tracker software version 3.10 was used to work with VICON; before each trial, four steps were taken. First, a *mask* had to be created to eliminate reflective objects that could lead to incorrect localization of the tracked object. As mentioned above, the elimination mask was always empty since the reflective objects were

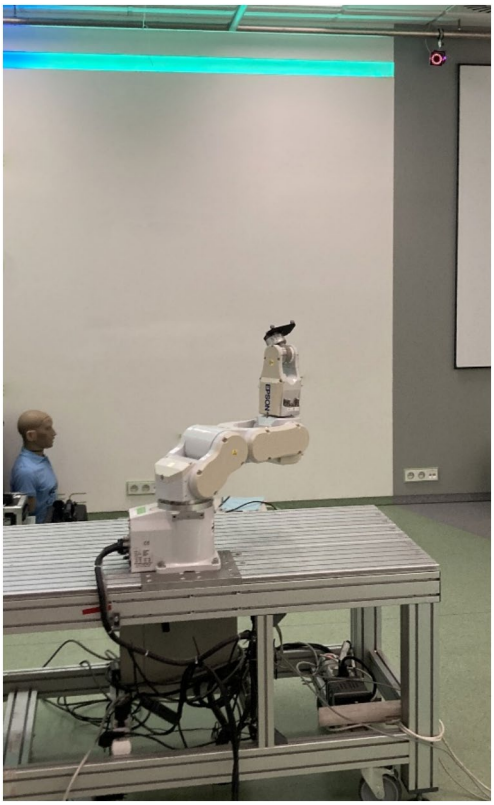

Fig. 2. The EPSON manipulator with a marker plate mounted at its endpoint.

absent in the room. Then, *calibration* was performed by moving the *wand* within the cameras' fields of view. Subsequently, the *centre T* was defined using the wand to determine the origin. In the final step, the tracked object had to be defined using visible markers.

Aligning the coordinate systems

After selecting the markers, VICON automatically computes the centre of gravity and orientation of the tracker, which is not aligned with the endpoint of the manipulator; thus, a transformation had to be computed and applied manually, according to Fig. 3.

In part (b) of this figure, the issue is illustrated with the manipulator shown in light blue and the markers in gray (M_A, M_B, M_C, M_D). The diagram includes all available dimension details. Information on the size of the plate and the grid was obtained from the Vicon documentation. The positions of the threads on the manipulator were obtained from the EPSON manipulator documentation. The distance of the marker plane to the endpoint plane represents the sum of half of the ball's radius and the plate's height, which is $h = 9.75$ mm.

Using geometric and trigonometric calculations, the positions applied to individual markers were determined. It is initially assumed that the coordinate systems will be rotated by -90 degrees along the Z_D axis, simplifying the calculations. Next, it is necessary to calculate the shifts along the X_D axis of the plate and the Y_D axis.

$$a = 15.75 \cdot sin\left(45 + tan\left(\frac{7}{21}\right)\right) = -14.08 \text{ mm}$$

$$b = 15.75 \cdot cos\left(45 + tan\left(\frac{7}{21}\right)\right) = -7.04 \text{ mm}$$

Using these shifts and the plate's grid, it is possible to calculate the positions of the markers for the given coordinate axis.

$$\begin{bmatrix} M_A \\ M_B \\ M_C \\ M_D \end{bmatrix} = \begin{bmatrix} x_A & y_A \\ x_B & y_B \\ x_C & y_C \\ x_D & y_D \end{bmatrix} = \begin{bmatrix} a & b+14 \\ a-42 & b+14 \\ a-42 & b-56 \\ a-14 & b-56 \end{bmatrix} = \begin{bmatrix} -14.08 & 21.04 \\ -56.08 & 21.04 \\ -56.08 & -48.96 \\ -0.08 & -48.96 \end{bmatrix}$$

All values are given in millimetres. Next, these positions need to be rotated around the axis Z_D by an angle θ, which is calculated using the following formula:

$\theta = -tan\left(\frac{7}{21}\right) - 90 = -109.47\ ^\circ$

The rotation is performed using a rotation matrix for all marker positions, as indicated in the previous equation:

$$\begin{bmatrix} M\prime_A \\ M\prime_B \\ M\prime_C \\ M\prime_D \end{bmatrix} = \begin{bmatrix} M_A \\ M_B \\ M_C \\ M_D \end{bmatrix} \boldsymbol{R}(\theta)^{\boldsymbol{T}} = \begin{bmatrix} -6.71 & 24.41 \\ -46.55 & 37.69 \\ -68.68 & -28.72 \\ -15.55 & -46.42 \end{bmatrix}$$

The resulting transformation is then applied to the tracker in Vicon software. It's important to keep in mind that the derived transformation is only valid under ideal conditions—which are impossible to achieve in practice

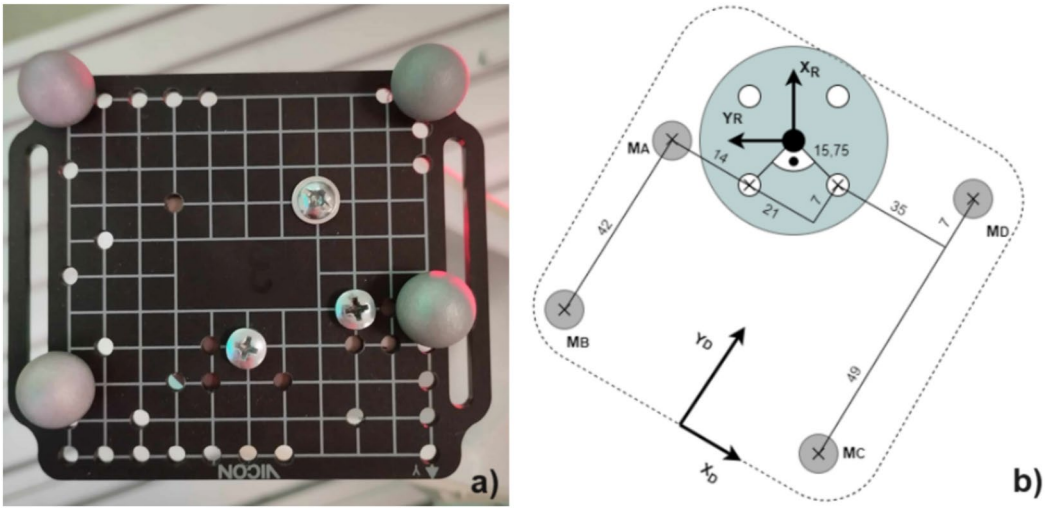

Fig. 3. Tracked object—plate with markers: (**a**) plate attached to the manipulator (**b**) diagram of the plate attached to the manipulator endpoint (light blue).

(e.g. due to clearance in mounting holes, etc.). For this reason, it is essential to perform a follow-up calibration, as described in the Data Preprocessing section.

Validation trajectories

Two validation trajectories were defined in the EPSON robot controller's scripting language SPEL+ (Fig. 4). The first trajectory, called positional, covered a hemisphere of 1.4 m diameter with no rotations, and the second trajectory, called rotational, covered the hemisphere with rotations with no translations. These trajectories were launched in several different places in the Covered Volume. During the execution of the trajectories, waiting intervals (*0.5* s) were inserted where the manipulator remained in the same position and rotation.

Capturing data

Recording of the VICON system and movement of the manipulator was launched simultaneously; the output from this measurement consisted of two records.

From the manipulator, a text file was obtained containing the coordinates of the tracker's position in millimetres, the rotation of the object represented in ZYX Euler angles in degrees, and two time intervals, indicating when the manipulator reached and leaved the given position. Since the robot controller is running the real-time OS, it is able to acquire the exact time of reaching and leaving each position in millisecond resolution.

The output from the VICON system is in X2D format, which had to be reloaded into the VICON Tracker software, where the data was subsequently exported to CSV format. During export, the rotation representation was set to quaternions. The file contains data on the coordinates of the object's position in millimetres and the rotation of the object in quaternions in each frame, with a sampling frequency of 100 Hz.

Data preprocessing

Due to the inability to achieve precise hardware-based time synchronization between the robot's data streams and the VICON system, and the impossibility of perfectly aligning the two coordinate systems during the design phase, the data need to be calibrated. The importance of preprocessing is significant, as even a small misalignment can introduce apparent errors into the validation results. However, a key advantage is that any error introduced during preprocessing can only degrade the results—it cannot make them appear better than they actually are. This is particularly important for our purposes, as we aim to quantify the worst-case accuracy of our setup.

The preprocessing was performed in the MATLAB software, consisting of three parts: *time synchronisation, axes calibration*, and *export of the resulting data*.

Time synchronisation was performed software-wise. The implementation was simplified thanks to the specific way the data was generated, where the manipulator always waited 0.5 s before executing a new command. The initial point was determined as the middle of the time interval where the manipulator maintained its set position. Subsequently, data from the VICON system was removed from the first and the last quarter of the waiting time, keeping the central half of the interval to eliminate transitional phenomenons. This was done for each time interval. With this procedure, we also ensured proper synchronization alignment by using the predefined dwell times of the EPSON controller and analysed VICON measurements only during these stationary intervals (not during movement phases). The dwell times were 2 times longer than the analysed periods to avoid misalignments. Moreover, any substantial misalignment would have manifested as outliers, which we did not observe, what is the proof of correct temporal synchronization.

Axes calibration was necessary even though the coordinate systems had already been roughly aligned earlier (see section Aligning the Coordinate Systems). This was due to imprecision of the standard Vicon calibration

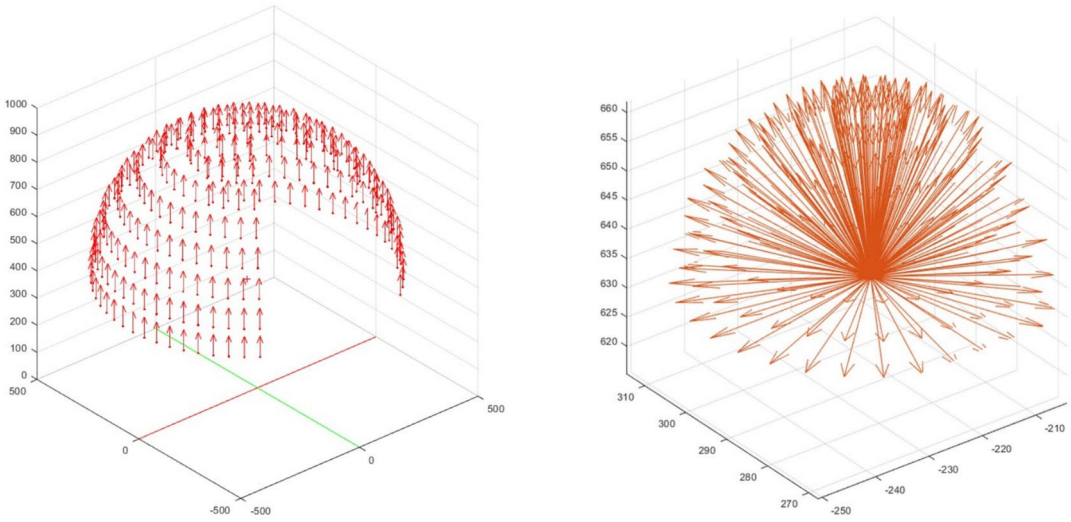

Fig. 4. Example of *positional* trajectory (left) and *rotational* trajectory (right) used for VICON accuracy validation.

procedure (prescribed by the manufacturer), and due to small deviations and clearances in the specific marker and how it was mounted.

As the experiment consisted of two separate datasets, a dedicated calibration was performed prior to each. Before each dataset, 287 static poses with constant orientation, covering the whole operational area of the manipulator, were collected. In each pose, the robot was moved to a known position, and the first available synchronized measurements from both the EPSON and VICON system were extracted.

The calibration can be divided into two parts: (1) aligning the coordinate systems of the manipulator and the Vicon system, and (2) aligning the coordinate system of the marker itself.

First, location values (e.g. X,Y,Z coordinates) of pose pairs were used to compute the rigid transformation between coordinate systems via Procrustes analysis[23] (*procrustes* in MATLAB, *with 'Scaling', false, 'Reflection', false*'), which was then applied to all captured points (during the calibration). The proper alignment was consequently verified using the mean residual error between the transformed VICON positions and the corresponding EPSON positions, yielding 0.2761 mm for Dataset 1 and 0.2932 mm for Dataset 2. These residuals are of the level of random errors further evaluated, thus confirming the proper alignment of the axes.

Second, it was also necessary to align the marker coordinate system. Although the VICON markers were mounted on a rigid plate fixed to the robot's end-effector, they were not located exactly at the tool centre point (TCP), nor necessarily aligned with its local coordinate axes. This fixed spatial offset and potential misalignment between the marker frame and the TCP frame can introduce a constant angular deviation in the measured orientations. To reliably estimate and correct this deviation, we continued with the calibrated data (see previous paragraph) and took the advantage of the fact that the orientation remained constant. Thus, we computed their average orientation in quaternion form and compare it to the true value (from the manipulator). The evaluated difference was added to the transformation, computed in the previous paragraph.

After completing both alignment steps, the actual experimental data were collected. The resulting constant transformation (combining both parts of the axes calibration) were then applied uniformly to all VICON data of the particular dataset.

In Fig. 5, a comparison of the individual position coordinates before and after applying the calculated transformation is shown. The graphs clearly demonstrate that the transformation successfully aligned both coordinate systems.

The final step was **data export**, where the final datasets for individual partial measurements were consolidated into CSV files. These files contain the position coordinates of the object in millimetres and rotations represented in ZYX Euler angles in radians from both VICON and the manipulator data.

Data analysis

All the accuracy analyses were performed using R environment with several packages, mainly psych[24], lme4[25], orientlib[26], and lmerTest[27]. Analytical scripts and data are publicly available at[28].

We computed the total Euclidean distance between the positions of VICON and EPSON as

$$d = \sqrt{(v_x + r_x)^2 + (v_y + r_y)^2 + (v_z + r_z)^2}$$

where v and r are the positions of the VICON motion capture system (v) and EPSON robot (r) on the x, y, or z axes in millimetres. Similarly, we computed the absolute angle between VICON and EPSON orientation in space using the *orientlib::rotation.distance* function and transformed the result to degrees. Both absolute distances and angles were thus positive.

As we assumed different precision in position and angle measurements across axes, we proceeded in several steps. First, we estimated the accuracy of distance and angle measurement for each axis separately. To separate

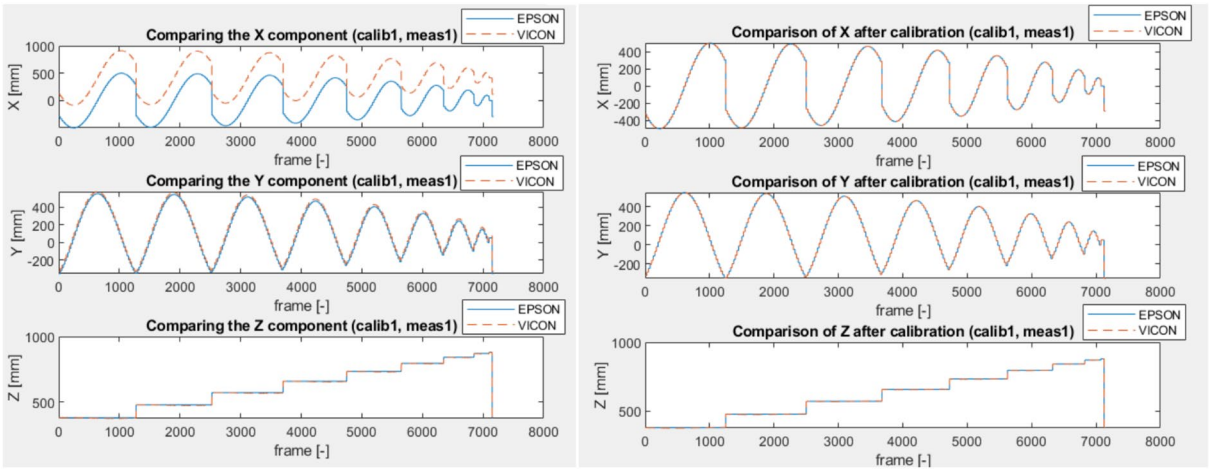

Fig. 5. Comparison of individual object position coordinates before (Left) and after (Right) applying the data calibration algorithm.

different sources of random errors (for example experiments, positions, or calibrations), account for the hierarchical structure of data, and isolate the systematic and random errors, we predicted the position of VICON motion capture system P_V using a linear mixed model (LMM)

$$P_V = \beta_1 P_E + \sum_{i=1}^{I} \gamma_i calib_i + \beta_3 type_r + \beta_4 \left(calib_2 \times type_r\right) + u_n + u_{pos} + \epsilon$$

with random effects

$$u_n \sim N\left(0, \sigma_n^2\right)$$
$$u_{pos} \sim N\left(0, \sigma_{pos}^2\right)$$
$$\epsilon \sim N\left(0, \sigma^2\right)$$

where fixed predictors were the position of the EPSON robot in millimetres (P_e), calibration ($calib$) with estimated parameters γ_1 and γ_2 for the first and second calibration, difference of rotational task from the positional ($type_r$), and the interaction of the second calibration with rotational tasks. Note that we omitted the intercept, so the calibration effect represented the average distance of VICON and EPSON within the first and second calibration. Finally, two random intercepts were included: the average distance between VICON and EPSON in each of the eight experiments (u_n), and the error of each measurement of the specific position (u_{pos}). The final term was random error (ϵ), representing random fluctuation of each VICON measurement at the specific position.

The significance of the fixed effect was tested using the robust Wald test with Satterthwaite's number of degrees of freedom, while the random effects were tested using likelihood-ratio tests (LRT) comparing the full model and the model with removed random effect. Effect sizes are reported using their raw values in millimetres (using standard deviations in random effects). We also report the absolute random error. Because the random terms are assumed to be normally distributed and they are orthogonal by design, it may be estimated as

$$SE = \sqrt{\sigma_n^2 + \sigma_{pos}^2 + \sigma^2}$$

The same approach and model specification were also used to determine the angle difference in degrees. Some of the models were singular, as the random effect was estimated to be numerically zero, which should not bias the rest of the parameters.

Tests of model assumptions (normality of residuals and random effects) showed heavy-tailed residual distributions across all models (high kurtosis), due to a large number of outliers. This may affect the reliability of standard errors and statistical tests; however, these are not the main focus of the study, and fixed-effect estimates remain robust. Residual variance may be slightly overestimated, potentially leading to underestimation of random effects, but given their small magnitude, the impact is likely negligible. To check the results, we also fitted robust LMMs using the robustlmm package[29]. However, estimates of fixed and random effects were nearly identical to those from the standard models.

Results

We report our results in three sections. First, we focus on systematic and random discrepancies between the position of the EPSON robot and the VICON MoCap within each of the three rotational or positional axes. Second, we report their correlations. Finally, we report the total errors: distances in space and angles' discrepancies.

Systematic and random errors within each dimension

Position

Systematic and random errors for position and each dimension separately are in Table 1. Calibration itself introduced small negligible errors < 0.1 mm. Moreover, the estimated position within rotational tasks slightly, but systematically, differed from that of positional tasks, < 0.4 mm, while this effect did not differ across types of tasks (all $p > 0.05$). Overall, all the systematic errors were negligible, with effect sizes below 0.4 mm.

Inspection of random effects revealed that the major source of random error was the effect of a specific position with a standard deviation across positions less than 0.5 mm. In other words, each real position (introduced by the EPSON robot) was observed as systematically biased by the VICON motion capture system. The fluctuation of each VICON measure within this position (residual) was negligible and less than 0.06 mm, while the systematic bias of each measured experiment was negligible (< 0.11 mm). The total random effect was still negligible, up to 0.46 mm within each dimension, and seems to be the major source of error.

Rotation

The systematic and random errors of rotation measurement are in Table 2. We excluded the real rotation (EPSON) about the z-axis from the model, as it was not manipulated and thus was constant. We see that all the systematic errors are negligible and below 0.1°, except a little bit of "upward" systematic bias of 0.42° within the rotational task and z-axis, but this is still negligible. In general, errors were slightly and significantly higher in rotational tasks, and especially in the second calibration (axes x and z), despite these effect sizes were very small.

The major random error was also caused, similarly as with the position, by the systematic bias within a specific position (u_{pos}). The difference between experiments was practically zero across all the dimensions.

	x – axis		y – axis		z – axis	
Fixed effects	**B (SE)**	**p**	**B (SE)**	**p**	**B (SE)**	**p**
EPSON (P_E)	1.00 (0.00)	< 0.001	1.00 (0.00)	< 0.001	1.00 (0.00)	< 0.001
Calibration 1 ($calib_1$)	0.00 (0.01)	0.886	− 0.04 (0.01)	0.002	− 0.09 (0.03)	0.005
Calibration 2 ($calib_2$)	0.00 (0.01)	0.727	− 0.04 (0.01)	0.003	− 0.08 (0.03)	0.006
Rotational task ($type_r$)	0.29 (0.02)	< 0.001	0.08 (0.02)	< 0.001	0.39 (0.02)	< 0.001
Calibration 2 × rotational task	0.02 (0.03)	0.471	− 0.01 (0.02)	0.710	0.03 (0.02)	0.291
Random effects	**SD**	**p**	**SD**	**p**	**SD**	**p**
Position (u_{pos})	0.46	< 0.001	0.40	< 0.001	0.35	< 0.001
Experiment (u_n)	0.00	< 0.001	0.00	< 0.001	0.01	0.384
Residual (ϵ)	0.06		0.05		0.05	
Total	0.46		0.40		0.35	

Table 1. Systematic and random error of space position for each dimension separately (millimetres). *Note.* All the variables are reported in millimetres. EPSON – position of the robot on the axis; calibration – systematic difference within the first or second calibration; rotational task – systematic difference of the rotational tasks from the spatial; experiment – systematic differences of the eight experiments; position (u_{pos}) – specific position within each of the experiments; residual – residual variance; total – root of sum-squared random effects, see the text for more information.

	x – axis		y – axis		z – axis	
Fixed effects	**B (SE)**	**p**	**B (SE)**	**p**	**B (SE)**	**p**
EPSON (P_E)	1.00 (0.00)	< 0.001	1.00 (0.00)	< 0.001	removed[a]	
Calibration 1 ($calib_1$)	0.00 (0.01)	0.879	− 0.01 (0.01)	0.521	0.00 (0.02)	0.884
Calibration 2 ($calib_2$)	− 0.01 (0.01)	0.699	0.00 (0.01)	0.703	0.01 (0.02)	0.581
Rotational task ($type_r$)	0.07 (0.03)	0.008	0.22 (0.02)	< 0.001	0.42 (0.02)	< 0.001
Calibration 2 × rotational task	0.10 (0.03)	0.001	− 0.02 (0.02)	0.487	0.07 (0.03)	0.034
Random effects	**SD**	**p**	**SD**	**p**	**SD**	**p**
Position (u_{pos})	0.48	< 0.001	0.38	< 0.001	0.52	< 0.001
Experiment (u_n)	0.00	0.914	0.00	0.911	0.00	1.000
Residual (ϵ)	0.10		0.08		0.12	
Total	0.49		0.39		0.53	

Table 2. Systematic and random error of rotation in space for each dimension separately (degrees). [a] Variable was constant by design and was removed from the model. *Note.* All the variables are reported in degrees. EPSON – position of the robot on the axis; calibration – systematic difference within the first or second calibration; rotational task – systematic difference of the rotational tasks from the spatial; experiment – systematic differences of the eight experiments; position (u_{pos}) – specific position within each of the experiments; residual – residual variance; total – root of sum-squared random effects, see the text for more information.

Residual (error within specific positions) was less than 0.13°. Overall, total random error was negligible, less than 0.54°. As with the positional tasks, random error was, on average, higher than systematic error introduced by calibration or by the type of task.

Dependency of bias across dimensions

The independence of errors across dimensions or between distance and rotation cannot be assumed. Therefore, we report Pearson's correlations across errors in Table 3. Note that these are raw correlations across all the experiments and positions, ignoring the multilevel structure of data. We report the correlations for all the measurements altogether and for different task types separately. There are some correlation patterns observed. For example, while the rotational error across the x and z axis was positive in the rotational task (r = 0.87), in the positional task was negative (r = −0.52). Another example is the negative correlation of rotational error at z-axis with position on y axis (r = −0.62) in positional tasks, which were rather small and positive in rotational tasks (r = 0.23); similar pattern is in x-position and y-rotation compared across positional (r = 0.67) and rotational (r = 0.00) tasks. However, the observed correlation can be attributed to the use of Euler angles, which are known to be non-unique and sensitive to singularities such as gimbal lock. In certain configurations, small changes in one angle (e.g., around the Z axis) can be compensated by changes in another (e.g., around the X axis), resulting in coupled errors. This inherent ambiguity and the nonlinear behaviour near singularities often lead to interdependent errors between axes. Nevertheless, we also stress that correlations do not imply the total error

All experiments						
	Position: x	Position: y	Position: z	Rotation: x	Rotation: y	Rotation: z
Position: x						
Position: y	0.003					
Position: z	0.137	0.237				
Rotation: x	0.095	0.237	0.341			
Rotation: y	0.052	0.143	−0.389	0.124		
Rotation: z	0.054	0.191	0.399	0.846	0.200	
Experiment types separately (positional above diagonal, rotational below diagonal)						
	Position: x	Position: y	Position: z	Rotation: x	Rotation: y	Rotation: z
Position: x		0.079	0.098	−0.135	−0.658	0.046
Position: y	−0.069		−0.242	0.096	0.059	−0.616
Position: z	−0.047	0.243		−0.370	−0.301	0.375
Rotation: x	0.014	0.227	0.268		0.005	−0.519
Rotation: y	0.003	0.163	−0.437	0.143		0.092
Rotation: z	−0.099	0.232	0.254	0.872	0.252	

Table 3. Pearson's correlations across errors. *Note.* Correlations $|r| < 0.006$ are not statistically significant. All the other correlations are significant at $p < 0.001$.

	Position [mm]					Rotation [deg]				
Type	*M*	*SD*	*Mde*	*min*	*max*	*M*	*SD*	*Mde*	*min*	*max*
Position	0.28	0.20	0.22	0.00	1.04	0.20	0.13	0.16	0.00	1.04
Rotation	1.03	0.37	1.06	0.09	2.47	0.61	0.39	0.52	0.02	2.00
Total	0.65	0.48	0.59	0.00	2.47	0.40	0.35	0.29	0.00	2.00

Table 4. Total error in space (distance and rotation).

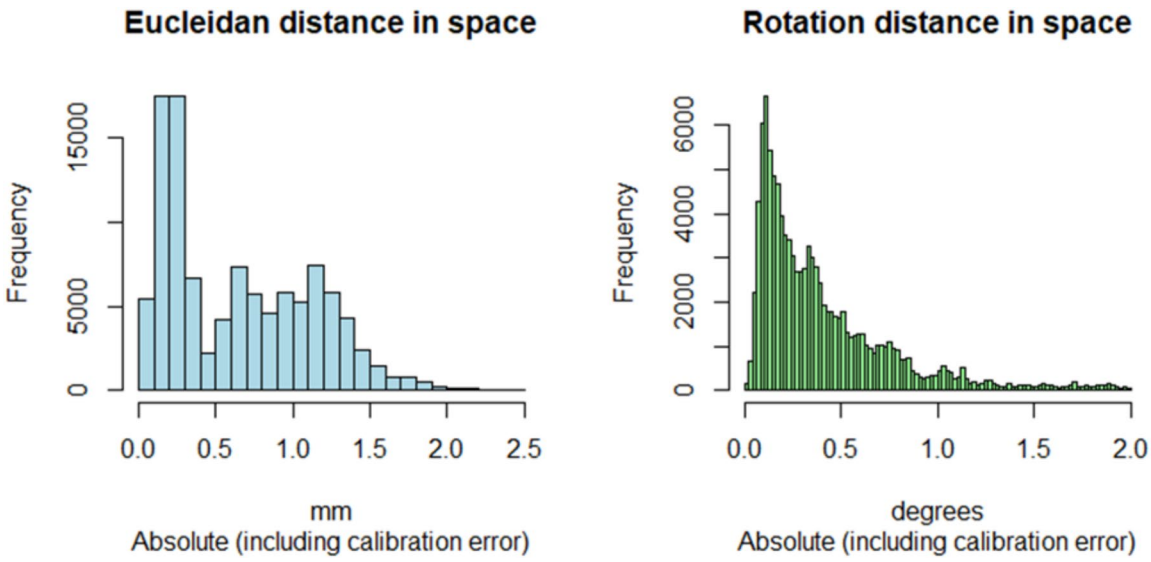

Fig. 6. Distribution of the total absolute discrepancy between EPSON and VICON positions.

size, which was different for rotational and positional tasks and for position and rotation and rather small in general. The total effect is, therefore, not even approximately an average of these two task types.

Total error

The total absolute discrepancy between EPSON and VICON positions is described in Table 4 and visualised using histograms in Fig. 6. We see that the total position error was small and below 0.65 mm on average. The error was of 0.75 mm higher for rotational tasks ($M = 1.03$, $SD = 0.37$ mm) compared to positional tasks ($M = 0.28$,

SD = 0.20 mm), which is in line with previous analyses within each axis separately. The maximal position error was less than 2.5 mm across all the experiments. The slightly bimodal distribution in distance error is caused by systematically higher error within rotational compared to positional tasks, as obvious from Tables 1 and 4.

The absolute angle in space between EPSON and VICON was also rather small, on average about 0.40°. On average, it was also here higher for about 0.41° in rotational tasks (M = 0.61, SD = 1.03°) compared to positional tasks (M = 0.20, SD = 0.13°).

Discussion

The average error in position across all the measurement was only 0.65 mm (SD = 0.48 mm) ranging in 0.00 – 2.47 mm out of the 1.4 m. The average rotational error was 0.40° (SD = 0.35) with the span of 0.00 – 2.00 degrees out of the 360°. Considering that the total area, where the MoCAP were tracking, covered $4.17 \times 3.45 \times 2.89$ m and we rotated the device all around, the error was completely negligible. Rotating the MoCAP device caused higher errors in both positions (0.75 mm) and rotations (0.41°).

We measured each position several time, and thus we could parcel the error introduced by the specific position and by each measurement. In both rotation and position, the random error within each position was negligible. On the other hand, an error specific to each position was much higher. We can conclude that some positions (both rotational or spatial) are harder to capture precisely, while others are quite easily measured. This can be caused in some specific poses by hiding some markers behind another one or being obscured by the manipulator's arm. Also the configuration, when two markers are so close in the view of a camera, that they are hardly distinguishable, may be influencing the accuracy. However, the error is included in the results of verification, and it was so small, that for the most purposes the error would not play any important role. Moreover, it is easily minimizable by adding more cameras[8].

There were some systematic differences in how both types of our experiments worked. First, in spatial experiment, the systematic source of error was significantly stronger. The calibration, type of task, or other systematic, non-random source of bias outperform the random fluctuations of measured position. On the other hand, within rotational tasks, the opposite was true, but with a small effect; random and systematic biased were much more comparable. This may be caused by the smaller number of problematic poses (see paragraph above) in the case of rotational experiment.

According to[5], calibration between individual measurements may play the role in the accuracy of the results. However, the effect of calibration is more than 20 times smaller than the abovementioned accuracy, thus negligible.

The reported static accuracy of our standardized setup (0.65 mm position error, 0.40° rotation error) aligns well with findings from recent inter-laboratory studies[7,30–32]. For instance, Schroeder et al.[33] compared several marker-based motion capture systems under static conditions and reported translational errors ranging from approximately 0.02 mm (GOM Pontos) to over 1 mm (CMS20), with commonly used systems like Vicon and OptiTrack achieving sub-millimeter accuracy in controlled laboratory environments. While those setups often relied on more advanced equipment or denser camera networks, our results were obtained using only five VICON VERO v1.3 cameras in a larger capture space ($4.17 \times 3.45 \times 2.89$ m), without the need for specialized or high-cost tools to operate the setup itself.

Although the validation was performed using a multi-marker tracker, the results related to positioning accuracy (excluding rotations) are also applicable to setups utilizing single-marker trackers. In fact, since the accuracy of a multi-marker tracker is affected by the relative placement of its markers—an additional source of error not present in the single-marker setup—it can be expected that the single-marker setup may achieve even higher accuracy than what is reported here.

Conclusion

The presented paper designed the standardized setup using the VICON motion-capturing system composed of the most popular VICON's cameras VERO v1.3, in the minimal configuration of 5 cameras. The setup design is based on the current state-of-the-art knowledge about the VICON system and its application in scientific research. The proposed setup is low-cost and affordable, fitting into the standard rooms, making the results of this paper widely usable.

Such a setup has been then verified in terms of accuracy. If the use of VICON MoCap does not differ from our setting, a user can expect that the measured position is, on average, 0.65 mm (SD = 0.48) far from the real position. The angle between the real and measured direction is, on average, 0.40° (SD = 0.35). For most types of use, such precision is sufficient, especially if we consider that the device rotated 360° around, within the area of $4.17 \times 3.45 \times 2.89$ m, which performs a relative accuracy of 0.01% in position and 0.11% in rotation (see section Results and Discussion for more details).

The key point of this paper is, that if the standardized setup is used and all its requirements are met, a similar accuracy of the specific setup as mentioned above can be expected without the need to revalidate the particular configuration. There is no need to perform any validation, thus no extra equipment (like robotic manipulator in our study) is needed.

Compared to existing MoCap validation approaches—which often rely on expensive multi-camera systems, custom robotic platforms, or precision linear actuators—this setup provides a simpler and more accessible solution, while still offering clearly quantified performance.

Moreover, using *exactly* this standardized setup is not the only way how to benefit from these results. According to[19] and[12], increasing the camera's resolution increases the accuracy of the whole system. This means that users with newer high-res VICON cameras can expect at least as good accuracy as above. It is not possible to conclude the accuracy of such a specific setup exactly, but knowing the worst-case accuracy is often sufficient information.

A similar conclusion can be made when adding more cameras to this standardized setup. According to[8], an increase in the number of cameras can lead to improved accuracy in the peripheral areas of the measured space; however, further improvement in accuracy in the main central part of the space can no longer be expected.

Although the proposed setup is designed to be easily reproducible, sometimes it can still be unattainable completely identically, and changes in certain environmental conditions may thus influence the overall accuracy. Therefore, maintaining the defined spatial configuration and avoiding sources of optical interference is recommended to achieve comparable results. The most essential is to maintain the manufacturer's recommendation on the environment (e.g. avoid strong changes in ambient lighting, reflective surfaces near the measurement space, flickering light sources, etc.) for proper marker recognition. In typical laboratory environments, this is usually easy to follow. It is good to reproduce the camera setup as close as possible, however, it has been observed that slight changes in the camera setup (like differences of camera placement up to 5 cm and their rotation displacement in the range up to 5°) plays negligible impact to the overall accuracy of the setup.

Finally, it is important to be aware that the characteristics mentioned above are exclusively static and cannot generally be used to infer the dynamic properties of the system. In real-world scenarios involving movement—especially in biomechanics or sports science—additional sources of error may arise, such as motion blur, marker occlusion, or tracking instability during fast or complex trajectories. While these effects were not evaluated in this study, certain elements of the proposed setup—such as overlapping camera views, close-range geometry, and the frontal camera minimizing occlusion—may help support reasonable tracking performance under moderate dynamic conditions. Nevertheless, when precise accuracy under motion is required, we recommend additional verification or reference to dynamic validation methods (more complex and more expensive), described in the scientific publications referenced at the beginning of this paper.

Data availability

All the source data and analytical scripts are publicly available form the OSF repository published at: https://osf.io/gzhbj/?view_only=a13cdee90a944d028d7e749b872d6f37.

Received: 3 December 2024; Accepted: 6 June 2025
Published online: 02 July 2025

References

1. Delbridge, M. *Motion Capture in Performance* (Palgrave Macmillan, 2015).
2. 3D motion capture system market size, share, industry report, revenue trends and growth drivers. Markets and Markets. (Accessed 9 August 2024). https://www.marketsandmarkets.com/Market-Reports/3d-motion-capture-system-market-193435109.html.
3. Menolotto, M. et al. Motion capture technology in industrial applications: A systematic review. *Sensors* **20**, 5687. https://doi.org/10.3390/s20195687 (2020).
4. Barrows, D. Videogrammetric model deformation measurement technique for wind tunnel applications. In *45th AIAA Aerospace Sciences Meeting and Exhibit* (ed. Barrows, D.) (American Institute of Aeronautics and Astronautics, 2007).
5. Windolf, M., Götzen, N. & Morlock, M. Systematic accuracy and precision analysis of video motion capturing systems—exemplified on the *Vicon-460* system. *J. Biomech.* **41**, 2776–2780. https://doi.org/10.1016/j.jbiomech.2008.06.024 (2008).
6. Yang, P.-F. et al. Evaluation of the performance of a motion capture system for small displacement recording and a discussion for its application potential in bone deformation in vivo measurements. *Proc. Inst. Mech. Eng. Part H J. Eng. Med.* https://doi.org/10.1177/0954411912452994 (2012).
7. Merriaux, P. et al. A study of Vicon system positioning performance. *Sensors* **17**, 1591. https://doi.org/10.3390/s17071591 (2017).
8. Aurand, A. M., Dufour, J. S. & Marras, W. S. Accuracy map of an optical motion capture system with 42 or 21 cameras in a large measurement volume. *J. Biomech.* **58**, 237–240. https://doi.org/10.1016/j.jbiomech.2017.05.006 (2017).
9. Hu, H. et al. Performance evaluation of optical motion capture sensors for assembly motion capturing. *IEEE Access* **9**, 61444–61454. https://doi.org/10.1109/ACCESS.2021.3074260 (2021).
10. Liu, H., Holt, C. & Evans, S. Accuracy and repeatability of an optical motion analysis system for measuring small deformations of biological tissues. *J. Biomech.* **40**, 210–214. https://doi.org/10.1016/j.jbiomech.2005.11.007 (2007).
11. Eichelberger, P. et al. Analysis of accuracy in optical motion capture – A protocol for laboratory setup evaluation. *J. Biomech.* **49**, 2085–2088. https://doi.org/10.1016/j.jbiomech.2016.05.007 (2016).
12. Diaz Novo, C. et al. The impact of technical parameters such as video sensor technology, system configuration, marker size and speed on the accuracy of motion analysis systems. *Ingeniería Mecánica Tecnol. Desarrollo* **5**, 265–271 (2014).
13. Carse, B. et al. Affordable clinical gait analysis: an assessment of the marker tracking accuracy of a new low-cost optical 3D motion analysis system. *Physiotherapy* **99**, 347–351. https://doi.org/10.1016/j.physio.2013.03.001 (2013).
14. Chiari, L. et al. Human movement analysis using stereophotogrammetry: Part 2: Instrumental errors. *Gait Posture* **21**, 197–211. https://doi.org/10.1016/j.gaitpost.2004.04.004 (2005).
15. Manecy, A. et al. X4-MaG: A low-cost open-source micro-quadrotor and its Linux-based controller. *Int. J. Micro Air Veh.* https://doi.org/10.1260/1756-8293.7.2.89 (2015).
16. Furtado, J. S. et al. Comparative analysis of OptiTrack motion capture systems. In *Advances in Motion Sensing and Control for Robotic Applications* (eds Janabi-Sharifi, F. & Melek, W.) 15–31 (Springer International Publishing, 2019).
17. Jang, S. et al. Comparison of camera based and inertial measurement unit based motion analysis. *Sensornets* https://doi.org/10.5220/0006716601610167 (2018).
18. Das, K., de Paula, O. T. & Newell, J. Comparison of markerless and marker-based motion capture systems using 95% functional limits of agreement in a linear mixed-effects modelling framework. *Sci. Rep.* **13**, 22880. https://doi.org/10.1038/s41598-023-49360-2 (2023).
19. How Accurate / Precise are your systems? Vicon. (Accessed 11 August 2024). https://www.vicon.com/support/faqs/how-accurate-precise-are-your-systems/.
20. Vicon Vantage cameras in a Vantage system - Vantage documentation - Vicon Help. (Accessed: 11 August 2024). https://help.vicon.com/space/Vantage/15053690/Vicon%C2%A0Vantage+cameras+in+a+Vantage+system.
21. Nagymate, G. & Kiss, R. Application of OptiTrack motion capture systems in human movement analysis a systematic literature review. *Recent Innov. Mech.* https://doi.org/10.17667/riim.2018.1/13 (2018).
22. Epson Robots. Epson C3 Compact 6-Axis RobotManual. (Accessed: 30 April 2014). http://robots.epson.com/admin/uploads/product_catalog /files/EPSON_C3_Robot_Manual(R7).pdf.
23. Gower, J. C. & Dijksterhuis, G. B. *Procrustes Problems* (Oxford University Press, 2004).
24. Revelle W. psych: Procedures for psychological, psychometric, and personality research. (2007).

25. Bates, D. et al. Fitting Linear Mixed-Effects Models Using lme4. *J. Stat. Soft.* https://doi.org/10.18637/jss.v067.i01 (2015).
26. Murdoch, D. Orientlib: An *R* package for orientation data. *J. Stat. Softw.* **8**, 1–11. https://doi.org/10.18637/jss.v008.i19 (2003).
27. Kuznetsova, A., Brockhoff, P. B. & Christensen, R. H. B. lmerTest package: Tests in linear mixed effects models. *J. Stat. Softw.* **82**, 1–26. https://doi.org/10.18637/jss.v082.i13 (2017).
28. Anonymized peer review link: https://osf.io/gzhbj/?view_only=a13cdee90a944d028d7e749b872d6f37.
29. Koller, M. Robustlmm: An *R* package for robust estimation of linear mixed-effects models. *J. Stat. Soft.* https://doi.org/10.18637/jss.v075.i06 (2016).
30. Johnson, J. D., Hales, M. & Emert, R. Validation of machine vision and action sport cameras for 3D motion analysis model reconstruction. *Sci. Rep.* **13**, 21015. https://doi.org/10.1038/s41598-023-46937-9 (2023).
31. Maggioni, V. et al. Optimisation and comparison of markerless and marker-based motion capture methods for hand and finger movement analysis. *Sensors* **25**, 1079. https://doi.org/10.3390/s25041079 (2025).
32. Robert-Lachaine, X. et al. Validation of inertial measurement units with an optoelectronic system for whole-body motion analysis. *Med. Biol. Eng. Comput.* **55**, 609–619. https://doi.org/10.1007/s11517-016-1537-2 (2017).
33. Schroeder, S. et al. Accuracy measurement of different marker based motion analysis systems for biomechanical applications: A round robin study. *PLoS ONE* **17**, e0271349. https://doi.org/10.1371/journal.pone.0271349 (2022).

Acknowledgements

The work has been performed in the project IMMAA: Imerzivita a automatizace pozemních bezpilotních prostředků (TQ03000946), which is co-funded with state support from the Technology Agency of the Czech Republic under the SIGMA Program. The work was supported by the infrastructure of RICAIP that has received funding from the European Union's Horizon 2020 research and innovation programme under grant agreement No 857306 and from Ministry of Education, Youth and Sports under OP RDE grant agreement No CZ.02.1.01/0.0/0.0/17_043/0010085.

We would also like to acknowledge the valuable contribution of an anonymous reviewer, whose suggestions led us to the discovery of an error in the alignment of coordinate systems between the VICON MoCap system and the EPSON C3 robotic manipulator. Based on these findings, we improved the alignment procedure, which significantly reduced the observed errors.

Author contributions

A. C. initiated the research idea, designed the experimental setup and coordinated and supervised the work. In this manuscript contributed to the Introduction and Conclusion section, reviewed the rest of the paper and finalized it. P. S. created the required software, performed experimental part including calibration, data acquisition, preprocessing and normalization. In this manuscript contributed to Material and Methods and Conclusion section. H. C. statistically evaluated the acquired data. In this manuscript contributed to the Materials and Methods, Results, Discussion and Conclusion section. All authors reviewed the manuscript. Petr Sopak created the required software, performed experimental part including calibration, data acquisition, preprocessing and normalization. In this manuscript contributed mostly to Material and Methods and Conclusion section. Hynek Cigler statistically evaluated the acquired data. In this manuscript contributed mainly to the Materials and Methods, Results, Discussion and Conclusion section.

Declarations

Competing interests

The authors declare no competing interests.

Additional information

Correspondence and requests for materials should be addressed to A.C.